Adsorption of Brilliant Green Dye Using Raw and Activated Adsorbent Prepared from Sesbania Leaves

Renu Yadav[1,], Anoop Kumar Sharma[2,] and Anil Yadav[3,*,]

[1]Department of Chemistry, Ahir College, Rewari-123401, India
[2]Department of Chemistry, Government PG College Rajgarh, Alwar-301408, India
[3]Department of Chemical Engineering, D.C.R. University Science and Technology, Murthal, Sonipat-131039, India

*Corresponding author: E-mail: anilyadav.che@dcrustm.org

In present study, the adsorption of brilliant green (BG) dye from an aqueous solution using raw sesbania leaves (RSL) and activated adsorbent of sesbania leaves (ACSL), batch adsorption studies were carried out to evaluate the effects of various parameters such as contact time, initial concentration, adsorbent dosage, pH and temperature on the removal of BG dye from aqueous solution. The maximum percentage removal of BG dye using RSL and ACSL was 73.2 and 93.8, respectively. The best-fitted isotherm for equilibrium data was Freundlich's and Langmuir's for ACSL and RSL adsorbents, respectively. The maximum adsorption capacities obtained were 158.74 mg/g and 98.41 mg/g for adsorption of BG dye on ACSL and RSL, respectively. The pseudo-second-order model best fit for the adsorption kinetic studies, which showed that the adsorption of BG dye on both adsorbents (RSL and ACSL) was limited by the chemisorption process. Thermodynamics parameters such as $(\Delta G°)$, $(\Delta H°)$ and $(\Delta S°)$ were also calculated. At 293 K to 333 K, the values of $\Delta G°$ lie in the range of 0.9346 to 1.1971 and 6.1199 to 9.0231 for RSL and ACSL, respectively, indicating that the adsorption process is spontaneous and endothermic.

Keywords: Activated adsorbent, Sesbania leaves, Isotherms, Brilliant green dye.

INTRODUCTION

Essential resources like clean air and water, which are crucial for human survival, are currently encountering unimaginable challenges. Water resources are polluted due to growth of industrial, mining and agricultural activities has much amount of organic and inorganic compounds pollutant including heavy metals, dyes, *etc.* [1-7]. Among, water contamination due to dyes discards from dyes industries are the major issues. It is estimated that 1.6 million dyes are produced annually to meet industrial demand with 10 to 15% of this volume being discarded as industrial effluent [8,9]. Discharged wastewater from these industries contains various types of colorant materials further mixed with underground and other water resources. So these types of wastewater contain dyes causes skin irritation, respiratory problem, brain damage, kidney problem, allergy, cancer and also mutation in human beings [10,11]. Therefore, elimination of these compounds from wastewater prior the community water uses is very most challenging. Hence, there

is an urgent requirement for development of cost-effective and efficient process for elimination of harmful dyes.

Various treatments techniques such as anaerobic and aerobic biological process [12,13], membrane filtration [14], ozonation, photocatalytic degradation, solvent extraction [15], electrochemical [16], adsorption [17], *etc*. Among of them adsorption has been found to be superior technique due to is cost effective, eco-friendly and easy to operate [18]. Various types of adsorbents such as natural, agricultural, industrial wastes and their prepared activated adsorbent in adsorption process are more attractive due to their easy availability, low-cost or no cost and minimum sludge production [19]. Previously researchers reported different type of low cost adsorbents and activated adsorbents such *Assalix alba* leaves [20], chemically modified areca nut husk [21], chemically activated date pit carbon [22], activated carbon prepared from waste banana peels [23], activated carbon derived from medlar seeds [24], activated carbon [25], Giombo persimmon seed [26], activated carbon prepared from flamboyant pod, eucalyptus tree, coconut shell and corn

cob [27] and nanohydroxyapatite/chitosan composite [28] for removal of brilliant green dye from wastewater.

Sesbania leaves, also known as raw sesbania leaves (RSL), is generally found throughout the Asian countries and is widely used in Ayurveda as a medicinal plant to regulate diabetes. The present study is focussed on the removal of textile dyes (brilliant green dye) from aqueous solution by the modification of Sesbania leaves (RSL) with conc. H_2SO_4. The effect of various operational parameters such as initial concentration, contact time and pH, isotherm models such as Langmuir, Freundlich, Temkin and Dubinin-Radushkevich (D-R) isotherms were evaluated. Kinetic parameters such as pseudo first order, pseudo second order and intraparticle diffusion model and thermodynamics parameters such as Gibb's free energy, change in the enthalpy and entropy change were also investigated. Thermodynamic investigation on the raw sesbania leaves (RSL) and activated sesbania leaf adsorbent (ACSL) reveal the nature and feasibility of brilliant green (BG) dye adsorption. A comparative studied of adsorption of BG dye on RSL and ACSL were also illustrated.

EXPERIMENTAL

Adsorbent collection and its preparation of activated adsorbent: The raw sesbania leaves (RSL) were collected from the vicinity of D.C.R. University of Science and Technology, Murthal, India. After being washed multiple times with double-distilled water to remove impurities and dust, the RSL was dried in an oven at 100 ºC for 24 h. The dried RSL was ground up in a household grinder and then sieved to a particle size of approximately 300 µ using a laboratory sieve shaker. The ground RSL maerial was subjected to an acid bath consisting of conc. H_2SO_4 at a ratio of 1:1 (w/v). It was ensured that the slurry form of powder precursor was thoroughly mixed before being stored for 48 h to allow for complete soaking of sulfuric acid on the RSL surface. In order to activate the slurry, it was baked in an oven at 600 ºC for 2 h [29]. The obtained extract (ACSL) was washed thoroughly multiple times with double-distilled water until the pH of solution becomes netural. The carbon obtained from RSL was dried in an oven at 105 ºC for 2 h. Subsequently, it was transferred into a tightly sealed bottle with a circular neck and an airtight closure.

Adsorbate and its stock preparation: Brilliant green dye (BG dye) was purchased from Lab Chemie (CAS no. 633-03-4) and the stock solutions of BG dye were prepared at a concentration 1000 mg/L and the aliquots were obtained by further diluting with double distilled water.

Batch adsorption experiment: Brilliant green (BG) dye is cationic in nature and used as adsorbate in the batch adsorption experiments, whereas RSL and ACSL were used as the adsorbents. The adsorption studies were also carried out to determine the effects of several parameters, including temperature (20, 30, 40, 50 and 60 ºC), contact time (20-140 min), initial BG dye concentration (10-100 mg/L), pH (2-10) and adsorbent dosage (5-50 mg). In batch experiments, 50 milliliters of a solution containing a fixed concentration of BG dye and 50 mg each of RSL and ACSL were shaken at 120 rpm using an orbital shaker. The mixture was left to settle at 30 ºC after 120

min of shaking. As a result, the BG dye-RSL and ACSL mixtures were centrifuged at 8000 rpm for 2 min to separate them and the separated liquid was then measured at 624 nm using a UV-visible spectrophotometer (Rigol-3000). The pH of the solution was kept constant using 0.1 N NaOH and 0.1 N HCl. Eqn. 1 was used to estimate the specific adsorption of BG dye in mg/g on RSL and ACSL at a particular period.

$$q_t = (C_o - C_t) \times \frac{V}{m} \tag{1}$$

where C_o and C_t (both in mg/L) are the initial dye concentration and after time t in the solution of BG dye; V (L) is the volume of solution; m (g) of RSL and ACSL.

Equilibrium studies: The adsorption isotherms (Langmuir, Freundlich, Temkin and Dubinin-Radushkevich isotherms) were investigated by establishing equilibrium (at 120 min) at 30 ºC. The calculation of adsorption capacity of BG dye was achieved by the simple mass balance (eqn. 2):

$$q_e = (C_o - C_e) \times \frac{V}{m} \tag{2}$$

The percentage removal of BG dye on RSL and ACSL, respectively was calculated using eqn. 3:

$$Dye\ removal\ (\%) = \frac{(C_o - C_e)}{C_o} \times 100 \tag{3}$$

where C_o and C_e (both in mg/L) are the initial and equilibrium concentration of BG dye, respectively; V (L) is the volume of solution, m (g) of RSL and ACSL.

Characterization of adsorbents: The FTIR analysis of RSL and ACSL samples were carried out by using Perkin-Elmer Frontier-BSEN60825, USA, instrument. The surface morphology of both adsorbents RSL and ACSL were characterized using a scanning electron microscopic (JEOL-6380, USA) technique. The X-ray diffraction analysis was used to provide information including identification and quantification of crystalline phases using X-ray diffractometer (Rigaku Miniflex, Japan). The pore size and surface area of RSL and ACSL were analyzed by Quanta Chrome Novae-2200, USA.

RESULTS AND DISCUSSION

Characterization of adsorbents: The SEM images of RSL and ACSL particles is shown in Fig. 1a-b. The RSL adsorbent had a number of irregular convolutions on the surface as shown in Fig. 1a. From the Fig. 1b, it can be observed that a well-aligned uniform pore network is developed upon activation, whereas the shape of some pore is spherical layer structure [30,31].

The FTIR of RSL and ACSL were analyzed in the range 4000-400 cm^{-1} as shown in Fig. 2a. In FTIR spectra, several functional groups *viz.* O-H, N-H, C-H, C=C, C-O and C-I exists on the surface of RSL and ACSL. In FTIR of RSL adsorbent, a peak at 3904 cm^{-1} represents the free stretching of O-H whereas a peak at 3458 cm^{-1} is attributed to the O-H stretching because of strong intermolecular bond. Another peak at 2127 cm^{-1} appears due to the strong stretching N=C=N bond, while at 1635 cm^{-1} appears due to the C=C stretching present in the alkene group on the RSL surface. A peak at 1416 cm^{-1} showed the bending
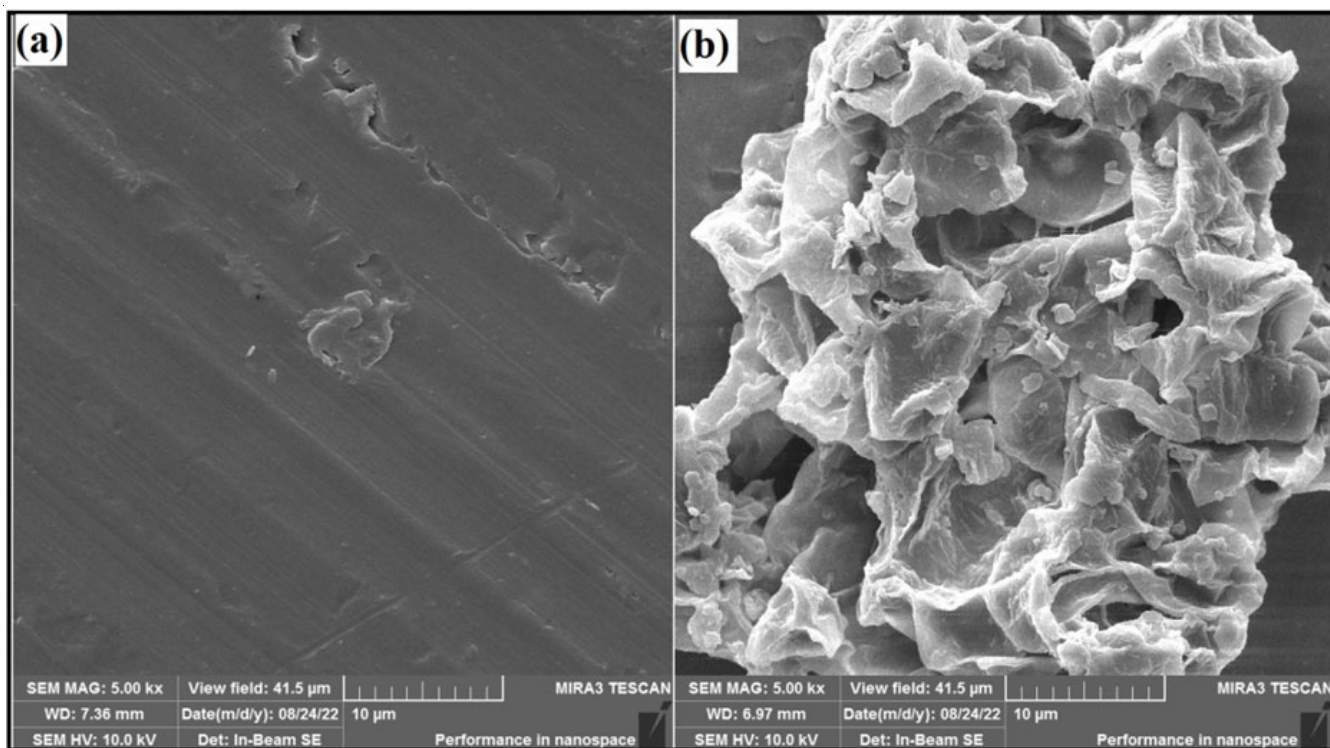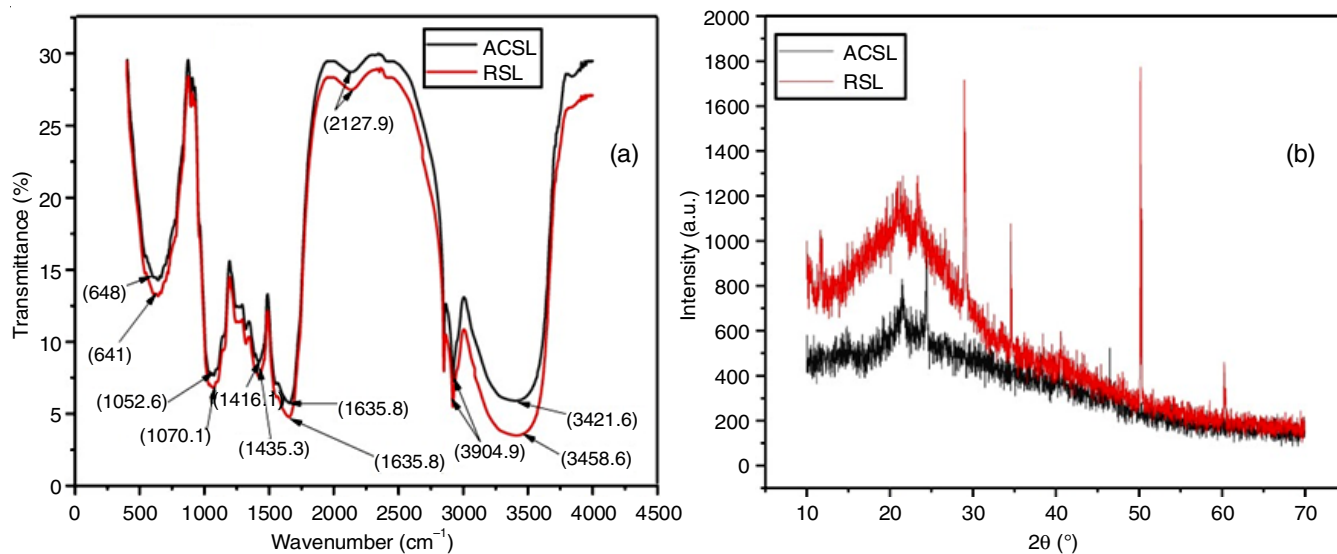
Fig. 1. (a) SEM image of RSL, (b) SEM image of ACSL

Fig. 2. (a) FTIR and (b) XRD spectra for RSL and ACSL adsorbents

O-H group, similarly the peaks at 1052 cm⁻¹ and 648 cm⁻¹ demonstrated the strong C-O stretching and strong C-I stretching functional groups, respectively on the surface of RSL adsorbents. The possible available active sites and structural changes follow after the activation of raw adsorbents (RSL) [29,32]. So, in ACSL adsorbent surface some peaks are new generated, shifted and disappeared, for example the peaks 3904 cm⁻¹ and 2127 cm⁻¹ are disappeared, whereas the peak at 3458 was shifted to 3421 cm⁻¹; 1416 cm⁻¹ to 1435 cm⁻¹; 1052 cm⁻¹ to 1070 cm⁻¹ and 648 cm⁻¹ to 641 cm⁻¹.

The XRD patterns of RSL and ACSL are shown in Fig. 2b. The characteristic diffraction peakes of RSL and ACSL at around 20º-25º were detected and showed no crystalline peak in the 10-70º scanning range thus indicating the amorphous phase of RSL and ACSL. The reason is attributed due to the arrangement of the glycosidic chain, which is hindered by join hydrogen bonding in the crystalline nature and a lack of such hydrogen bonding in the amorphous nature following the preparation of activated adsorbent of adsorbents [29,33].

Adsorption studies

Effect of initial concentration: The concentration of BG dye adsorption onto RSL and ACSL at various initial concentrations between 50 and 100 mg/L at pH 4 and 7 for 120 min

is shown in Fig. 3b. The adsobed amount of BG dye ranges from 5.83 mg/g and 7.92 mg/g to 61.9 mg/g and 89.84 mg/g of RSL and ACSL at 10 mg/L and 100 mg/L, respectively (Table-1). The percentage of removal for BG dye initially increased (not shown in graph) and then decreased, which may be related to the fact that sufficient adsorption at a lower concentration facilitates the BG dye interaction with several vacant active sites on RSL and ACSL adsorbents were available. However, once the vacant active sites became saturated, it was challenging to attract more the BG dye molecules due to repulsive forces exerted by the adsorbate molecules [17,34].

TABLE-1
AMOUNT ADSORBED OF BRILLIANT GREEN DYE AT DIFFERENT INITIAL DYE CONCENTRATION ON RSL AND ACSL

Initial concentration (mg/L)	Amount adsorbed (mg/g)	
	RSL	ACSL
10	5.83	7.92
20	13.16	17.12
30	20.52	26.55
40	29.04	36.68
50	36.60	46.90
60	42.78	55.76
70	48.51	64.65
80	54.00	73.14
90	57.78	81.61
100	61.90	89.84

Effect of contact time: The effect time of the elimination of BG dye using RSL and ACSL at concentrations of 50 mg/L and pH 7 and 4, respectively is shown in Fig. 3a. The amount adsorbed of BG dye at different contact time (20 to 140 min) on RSL and ACSL are revealed on Table-2. The amount adsorbed

TABLE-2
AMOUNT ADSORBED OF BRILLIANT GREEN DYE AT DIFFERENT TIME ON RSL AND ACSL

Contact time (min)	Amount adsorbed (mg/g)	
	RSL	ACSL
20	27.30	34.40
40	29.45	38.95
60	31.25	41.75
80	33.90	43.90
100	35.25	45.80
120	36.60	46.90
140	36.60	46.90

36.6 mg/g and 46.9 mg/g of RSL and ACSL at 120 min with 50 mg/L BG dye concentration. Intially only 60-70% removal of BG dye was achieved at the half time and thus thereby extending the contact time. This might be because, as contact time increased more vacant active sites at the RSL and ACSL surface became available, and the percentage of BG dye removed was rapidly increasing at the initial stage of the absorption process [34,35]. At 120 min, it was found that the maximum percentages of BG dye removed using RSL and ACSL adsorbents were 73.2% and 93.8%, respectively.

Effect of dosage: Effect of different amounts of adsorbents on the adsorption of brilliant green dye is shown in Fig. 3c, while kept the other parameters optimized. The percentage removal of BG dye were achieved within 18.7 to 73.2% and 28.9 to 93.8% for RSL and ACSL, respectively (Table-2). It was observed that an increase in the accessible active sites caused the adsorption to increase along with the dosage of the adsorbents [35,36].

Effect of pH solution: The BG dye adsorption experiments was conducted at wide range of pH from 1 to 10 while
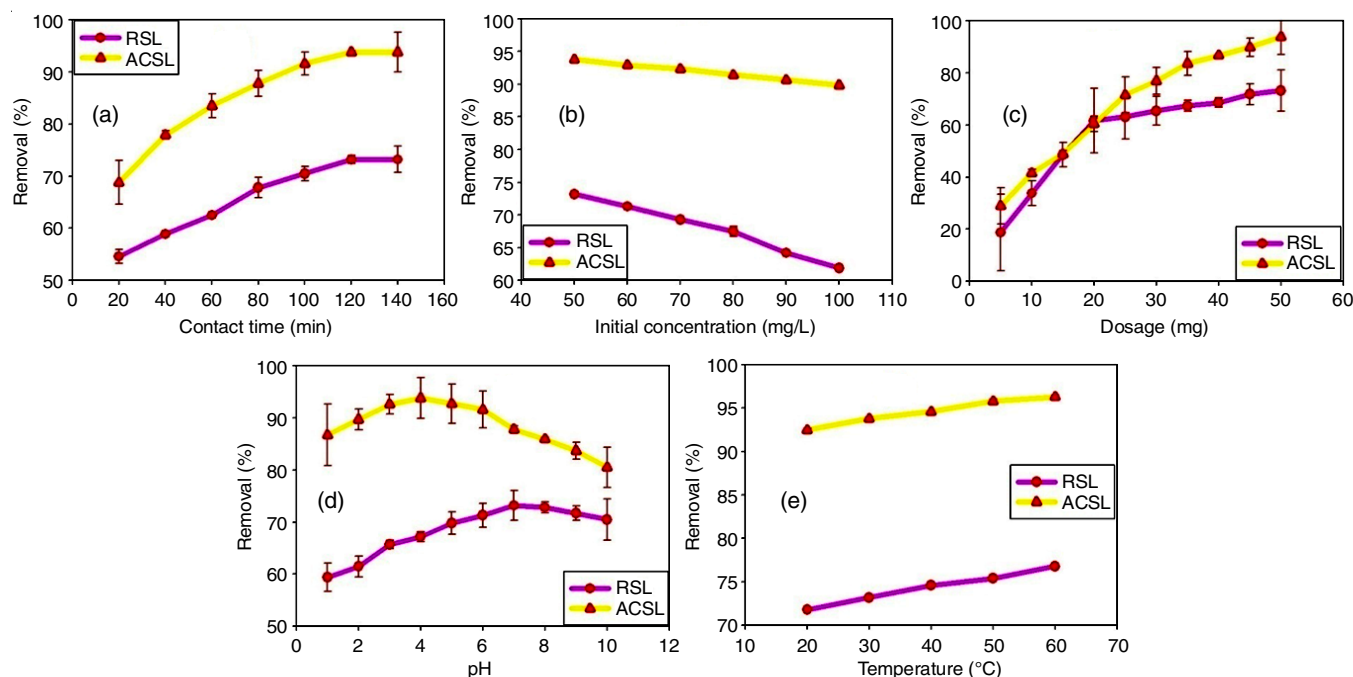

Fig. 3. (a) Influence of contact time, (b) Influence of initial concentration, (c) Influence of RSL and ACSL dosages, (d) Influence of pH and (e) Influence of temperature (Following conditions: concentration = 50 mg, contact time = 120 min, adsorbent, temperature = 30 °C, dosage = 50 mg, pH = 7 for RSL, pH = 4 for ACSL)

keeping the other conditions like dosage of RSL and ACSL (50 mg), BG concentration (50 mg/L), contact time (120 min), temper-ature (30 ºC) and volume of sample (50 mL) optimized. Fig. 3d clearly demonstrated the maximum percentage removal of BG dye on RSL = 73.2% at pH = 7 and ACSL = 93.8% at pH = 4. So, it is concluded that pH = 7 and pH = 4 were the optimum conditions for the adsorption of BG dye on RSL and ACSL, respectively. It was also observed that slow increase in the percentage of removal occurs due to the large concentration of hydrogen ions in the solution, which occupy the active sites when the pH falls within the range of 1 to 4. At higher pH range from 4 to 7, ACSL surface gain negatively charges on higher pH due to this reason possibility increases the more attraction between the cationic dye and ACSL along with the electrostatic forces of attraction than RSL surfaces [20,23,37]. Due to the occupation of the active sites by hydrogen ions, both adsorbents (RSL and ACSL) repels the BG dye cations ions, leading to the lower adsorption.

Adsorption isotherms: Adsorption isotherms are useful technique for understanding adsorbent surface features, as well as for establishing an adsorption process and determining the adsorbent capacity [16]. In this work, four different isotherms *viz.* Langmuir, Freundlich, Temkin and D-R isotherms models were used to study the equilibrium adsorption of BG dye on RSL and ACSL.

Langmuir adsorption isotherm: The Langmuir isotherm assumes that monolayer coverage of adsorbent and adsorption occurs over homogeneous active sites on the adsorbent. The linear form of the Langmuir isotherm is expressed as eqn. 4 [7]:

$$\frac{C_e}{q_e} = \left(\frac{1}{K_L q_m} + \frac{C_e}{q_m} \right) \qquad (4)$$

where K_L (L/mg) and C_e (mg/L) are the Langmuir constant and equilibrium concentration of BG dye, respectively; q_e (mg/g) represents the adsorbed capacity at equilibrium.

The feasibility of adsorption on adsorbent can be expressed by the separation factor (R_L) related to Langmuir isotherm. It is a dimensionless parameter and can be calculated by eqn. 5:

$$R_L = \frac{1}{(1 + K_L C_o)} \qquad (5)$$

The value of K_L and q_m were calculated from the plot of BG dye (figure not shown) and their values are shown in Table-3. The R^2 values for the removal of BG dye on RSL and ACSL were 0.9973 and 0.9958, respectively. Thus, the monolayer adsorption capacity for adsorption of BG dye on RSL and ACSL were 98.41 mg/g and 151.74 mg/g, respectively and the separation factor (R_L) values were found to be 0.3082 and 0.1254 for RSL and ACSL, respectively. The R_L value for both RSL and ACSL between 0 and 1, gives the favourability of the adsorption process [10,38].

Freundlich adsorption isotherm: Freundlich isotherm is used to describe the multilayer adsorption on heterogeneous surface and adsorption capacity of dye at equilibrium concentration. The linear form of Freundlich type isotherm can be expressed as eqn. 6:

TABLE-3
LANGMUIR'S, FREUNDLICH'S, TEMKIN'S AND DUBININ-RADUSHKEVICH ISOTHERM CONSTANTS FOR THE ADSORPTION OF BRILLIANT GREEN DYE ON RSL AND ACSL

Model	Adsorbents	RSL	ACSL
Langmuir's	q_e (mg/g)	98.41	151.74
	K_L (L/mg)	0.0449	0.1395
	R_L	0.3082	0.1254
	R^2	0.9973	0.9958
Freundlich's	1/n	0.5012	0.5496
	n	1.9951	1.8194
	K_F (mg/g)	2.7444	4.0697
	R^2	0.9863	0.9988
Temkin's	A_T (L/mg)	0.3404	1.1270
	B	24.2912	36.3167
	R^2	0.9967	0.9949
Dubinin Radushkevich	q_s (mg/g)	63.9436	89.4151
	K_{ad} (mol²/kJ²)	9.0051×10^{-6}	1.4164×10^{-6}
	E (kJ/mol)	0.2356	0.8402
	R^2	0.9681	0.9306

$$\log q_e = \log K_f + \frac{1}{n} \log C_e \qquad (6)$$

where K_f (mg/g) degree of sorption and 1/n intensity of adsorption were obtained from the intercept and slope log q_e *versus* log C_e. The value of n greater than one indicated that the adsorption isotherm is favourable [38]. The values of K_f and 1/n of adsorption of BG dye on RSL and ACSL and their values are given in Table-3.

Temkin adsorption isotherm: Temkin adsorption isotherm gives the idea of interactions between adsorbate and adsorbent. This isotherm also explains that the heat of adsorption of all molecules layer, decrease linearly with the coverage involved in this interaction. The Temkin isotherm can be expressed in the form of eqn. 7 as:

$$q_e = B \ln A_T + B \ln C_e \qquad (7)$$

where A_T (l/mol) and B are the equilibrium binding energy and heat of adsorption, respectively determine from the intercept and the slope of the graph between q_e *versus* ln C_e. The R^2 values were found to be 0.9967 and 0.9949 for adsorption of BG dye on RSL and ACSL, respectively.

Dubinin-Radushkevich (D-R) adsorption isotherm: The Dubinin Radushkevich (D-R) adsorption model is used to study the apparent free energy and characteristics of adsorption. The linearized form of D-R adsorption isotherm is given by eqn. 8 [19]:

$$\ln q_e = \ln q_m - (\beta \epsilon^2 2) \qquad (8)$$

where q_m (mg/g) is the D-R isotherm adsorption capacity and β (mol²/kJ²) is D-R isotherm constant and ϵ (J/mol) is the Polyani potential which can be calculated by using eqn. 9:

$$\epsilon = RT \ln \left(1 + \frac{1}{C_e} \right) \qquad (9)$$

The value of mean free energy (E) can be calculated by following eqn. 10:

$$E = \frac{1}{\sqrt{(-2\beta)}} \qquad (10)$$

The E values are crucial parameters in the D-R isotherm for determining the types of adsorption, namely physical and chemical adsorption. The E is lower than 8 kJ/mol, physical adsorption dominates and if the value of E is in range 8 to 16 kJ/mol, the adsorption process explained the chemical adsorption [32,38]. In this study, the values of E obtained were 0.2356 and 0.8402 for adsorption of BG dye on RSL and ACSL, respectively, which indicate that the physical adsorption in both adsorbents [32]. The correlation coefficients R^2 of D-R isotherm were 0.9306 and 0.9681 for adsorption of BG dye on ACSL and RSL, respectively. Since, the applicability of various isotherms for the adsorption of BG dye on RSL and ACSL was obtained by the correlation coefficient R^2, it is concluded that best fitted Freundlich and Langmuir adsorption isotherm for adsorption of BG dye on RSL and ACSL, respectively.

Adsorption kinetic models: The kinetic models for the adsorption of brilliant green dye on RSL and ACSL were also investigated. To determine the kinetic mechanism for the adsorption of brilliant green dye on RSL and ACSL, the linear form of pseudo-first order, pseudo-second order and the intraparticle diffusion model were evaluated by using eqns. 11-13, respectively [39].

$$\ln(q_e - q_t) = \ln q_e - \frac{K_1}{2.303} t \tag{11}$$

$$\frac{t}{q_t} = \left(\frac{1}{K_2 q_e^2} + \frac{1}{q_e t} \right) \tag{12}$$

$$q_t = K_{id} t^{0.5} + C \tag{13}$$

where K_1 (min^{-1}), K_2 (g mg^{-1} min^{-1}) and K_{id} (mg g^{-1} min$^{-0.5}$) are the rate constant pseudo first order, pseudo second order and intraparticle diffusion, respectively; q_e (mg/g) and q_t (mg/g) are adsorption capacity at equilibrium and any time (t), respectively; C is the intercept. Based on the kinetic adsorption parameters (Table-4), the highest value of R^2 in the pseudo second order adsorption model for RSL and ACSL indicate the best fitting of the data and adsorption of BG dye on RSL and ACSL follows pseudo-second order model. Moreover, these results demonstrated that the adsorption of BG dye on both adsorbents confirms the chemisorption process [32].

The intraparticle diffusion provides a feasible mechanism by which the adsorption of BG dye on RSL and ACSL occurs as a function of time contact. Since the adsorbent has a porous structure, the adsorption process can occur at different stages, such as external mass transfer, adsorption onto actives sites and inner diffusion of the adsorbate into the pores. The intraparticle diffusion parameters and their correlation coefficient (R^2) for adsorption of BG dye on RSL and ACSL are shown in Table-4. For intraparticle diffusion, the plot of q^t against $t^{0.5}$ (figure not shown) will be linear passing through origin and if not linear, then some other mechanism may also be involved. If the graph exhibits non-linearity throughout the entire time interval, it indicates that the adsorption of BG dye on RSL and ACSL was influenced by more than one process [32].

Effect of temperature study and adsorption thermodynamic parameters: The adsorption of adsorption of BG

TABLE-4
SUMMARY OF PARAMETERS FOR VARIOUS KINETIC MODELS AND THERMODYNAMICS PROPERTIES FOR BG DYE ON RSL AND ACSL

Kinetic model	Parameters	RSL	ACSL
Pseudo first-order	q_e (mg g^{-1})	17.8789	25.4567
	K_1 (min)$^{-1}$	0.0557	0.0672
	R^2	0.9509	0.9637
Pseudo second-order	q_e (mg g^{-1})	39.8991	50.8135
	K_2 (g mg^{-1} min^{-1})	0.0019	0.0017
	R^2	0.9969	0.9991
Intra-particle diffusion	K_{id} (g mg^{-1} min$^{-0.5}$)	1.3819	1.7512
	C (mg g^{-1})	21.0079	27.5782
	R^2	0.9809	0.9663
Thermodynamic Properties	$\Delta H°$ (kJ mol^{-1})	5.1939	15.440
	$\Delta S°$ (kJ mol^{-1} K^{-1})	25.1971	73.5069
	R^2	0.9942	0.9907
	$-\Delta G° \times 10^2$ (kJ mol^{-1})		
	293 K	0.9346	6.1199
	303 K	1.0048	6.8435
	313 K	1.0774	7.4510
	323 K	1.1201	8.3978
	333 K	1.1971	9.0231

dye on RSL and ACSL were studied at different temperatures such as 293 K, 303 K, 313 K, 323 K and 333 K. By increasing the temperature range from 293 K to 333 K, the percentage removal of brilliant green dye increases from 71.8% to 76.8% and 92.5% to 95.6%, for RSL and ACSL, respectively. This would be occurring due to main three reasons (i) increase in temperature leads to high diffusion rate of adsorption of BG dye on RSL and ACSL molecules across external mass transfer surface, (ii) at lower solution temperatures, BG molecules have less mobility, which means that there is less interaction between the dye molecules and the active sites of RSL and ACSL, leading to a lower removal percentage; (iii) when increase the temperature of solution, number of vacant active sites for adsorption are increased due to the breakdown of the internal bonds of adsorbents [40].

Thermodynamics parameters including Gibb's free energy ($\Delta G°$), enthalpy change ($\Delta H°$) and entropy change ($\Delta S°$) can be investigated by using Langmuir isotherm eqns. 14, 15 and van't Hoff plots eqn. 16 [41].

$$K_c = \frac{C_e}{C_o - C_e} \tag{14}$$

$$\Delta G° = -RT \ln K_c \tag{15}$$

$$\ln K_c = \left(\frac{\Delta S°}{R} - \frac{\Delta H°}{RT} \right) \tag{16}$$

where C_o and C_e are concentration at initial and equilibrium of dye (mg/L); K_c is the Langmuir's equilibrium constant (L/mg); R (8.314 J/mol K) is the universal gas constant and T is the temperature in K. The $\Delta H°$ and $\Delta S°$ values were obtained from slope and intercept of ln K_c *versus* 1/T (figure not shown). The thermodynamic parameters data estimated for 50 mg/L of BG dye at contact time 120 min are shown in Table-4. The negative value of $\Delta G°$ shown in Table-4 indicates the feasibility and spontaneous nature of adsorption of BG dye on RSL and

TABLE-5
SUMMARIES THE MAXIMUM ADSORPTION CAPACITY OF ADSORPTION
OF BRILLIANT GREEN DYE WITH VARIOUS ADSORBENTS

Adsorbents	Maximum adsorption capacities (mg/g)	Reference
Activated carbon prepared from flamboyant pod	0.0014	[27]
Activated carbon prepared from corn cob	0.0014	[27]
Activated carbon prepared from eucalyptus tree	0.0015	[27]
Activated carbon prepared from coconut shell	0.008	[27]
Saklikent mud	1.18	[43]
Acronseed shell carbon	2.11	[44]
Salix alba leaves	8.47	[20]
Areca nut husk carbon	18.21	[21]
Saw dust from eucalyptus with NaOH treated	58.48	[45]
Kaolin	65.42	[46]
Guava tree carbon	90	[37]
Composite snail shell and rice husk	129.87	[47]
RSL	98.41	Present study
ACSL	151.69	Present study

ACSL, respectively. The value of ΔH° is less than 40 kJ/mol represents the physisorption and adsorption process is endothermic [41]. The positive value of ΔS° shown in Table-4 confirmed that the feasibility of adsorption process and increasing randomness at the adsorbent-solution interface during adsorption of BG dye onto the vacant active sites of RSL and ACSL [42].

Comparison of adsorption capacity of RSL and ACSL with other studies: By considering the significant maximum adsorption capacity of RSL and ACSL for the removal of brilliant green (BG) dye, in the present work, efforts have been taken to compare removal efficiency with other reported adsorbents. Table-5 shows the comparison data of maximum adsorbents capacities of other adsorbents reported in literature for the BG dye removal.

Conclusion

The activated adsorbent of raw sesbania leaves (RSL) was successfully prepared from RSL using chemical activation method. Both RSL and ACSL exhibited great efficiencies in the brilliant green (BG) dye removal from the aqueous solution. The various parameters such as contact time, initial concentration, amount of adsorbent, temperature were also optimized in order to achieve the maximum removal percentage and adsorption capacity. The maximum percentage removal of BG dye using RSL and ACSL were 73.2% and 93.8%, respectively. The adsorption equilibrium data were best fitted to Freundlich and Langmuir adsorption isotherms for adsorption of BG on ACSL and RSL, respectively. The kinetic data of adsorption of BG dye using RSL and ACSL follows the pseudo-second order adsorption kinetic models. The randomness for the adsorption of BG dyes using RSL and ACSL, increases with increase in the temperature, which shows spontaneous and endothermic process. Moreover, the adsorption of BG dye using RSL and ACSL as adsorbents was found to be better as compared other reported agricultural waste materials.

CONFLICT OF INTEREST

The authors declare that there is no conflict of interests regarding the publication of this article.

REFERENCES

1. A. Ouni, N. Rabaaoui, L. Mechi, N. Enaceur, A.K.D. AlSukaibi, E.M. Azzam, K.M. Alenezi and Y. Moussaoui, *J. Saudi Chem. Soc.*, **25**, 101326 (2021);
https://doi.org/10.1016/j.jscs.2021.101326

2. J.R. Sunkara and S.M. Botsa, *Chem. Africa*, **2**, 635 (2019);
https://doi.org/10.1007/s42250-019-00086-7

3. H. Elhleli, F. Mannai, M.B. Mosbah, R. Khiari and Y. Moussaoui, *Processes*, **8**, 1242 (2020);
https://doi.org/10.3390/pr8101242

4. V. Kumar, M. Sharma, S. Sondhi, K. Kaur, D. Sharma, S. Sharm and D. Utreja, *Sustainability*, **15**, 16376 (2023);
https://doi.org/10.3390/su152316376

5. I. M'barek, M. Gun, Y. Moussaoui, H. Arslan and N. Dizge, *Int. J. Environ. Sci. Technol.*, **20**, 4839 (2022);
https://doi.org/10.1007/s13762-022-04435-x

6. F. Taleb, M. Ammar, M. Mosbah, R. Salem and Y. Moussaoui, *Sci. Rep.*, **10**, 11048 (2020);
https://doi.org/10.1038/s41598-020-68047-6

7. M. Ben Mosbah, A.K.D. Alsukaibi, L. Mechi, F. Alimi and Y. Moussaoui, *Water*, **14**, 1509 (2022);
https://doi.org/10.3390/w14091509

8. M. Naushad, T. Ahamad, Z.A. AlOthman and A.H. Al-Muhtaseb, *J. Mol. Liq.*, **279**, 1 (2019);
https://doi.org/10.1016/j.molliq.2019.01.090

9. Y. Zhou, J. Lu, Y. Zhou and Y. Liu, *Environ. Pollut.*, **252**, 352 (2019);
https://doi.org/10.1016/j.envpol.2019.05.072

10. V. Yadav, D.P. Tiwari and M. Bhagat, *Asian J. Chem.*, **30**, 2765 (2018);
https://doi.org/10.14233/ajchem.2018.21611

11. N. Sivarajasekar, R. Baskar, T. Ragu, K. Sarika, N. Preethi and T. Radhika, *Appl. Water Sci.*, **7**, 1987 (2017);
https://doi.org/10.1007/s13201-016-0379-2

12. J. García-Montaño, X. Domènech, J.A. García-Hortal, F. Torrades and J. Peral, *J. Hazard. Mater.*, **154**, 484 (2008);
https://doi.org/10.1016/j.jhazmat.2007.10.050

13. E. Hosseini Koupaie, M.R. Alavi Moghaddam and S.H. Hashemi, *J. Hazard. Mater.*, **195**, 147 (2011);
https://doi.org/10.1016/j.jhazmat.2011.08.017

14. E. Alventosa-deLara, S. Barredo-Damas, M.I. Alcaina-Miranda and M.I. Iborra-Clar, *J. Hazard. Mater.*, **209–210**, 492 (2012);
https://doi.org/10.1016/j.jhazmat.2012.01.065

15. C. Prasse, D. Stalter, U. Schulte-Oehlmann, J. Oehlmann and T.A. Ternes, *Water Res.*, **87**, 237 (2015);
https://doi.org/10.1016/j.watres.2015.09.023

16. B.K. Körbahti, K. Artut, C. Geçgel and A. Özer, *Chem. Eng. J.*, **173**, 677 (2011);
https://doi.org/10.1016/j.cej.2011.02.018

17. M. Sharma, R.K. Vyas and K. Singh, *Adsorption*, **19**, 161 (2013);
https://doi.org/10.1007/s10450-012-9436-9

18. Y. Shi, S. Zhong, X. Wang and C. Feng, *Desalination Water Treat.*, **286**, 238 (2023);
https://doi.org/10.5004/dwt.2023.29340

19. A.N.M.A. Haque, N. Sultana, A.S.M. Sayem and S.A. Smriti, *Sustainability*, **14**, 11098 (2022);
https://doi.org/10.3390/su141711098

20. R. Fiaz, M. Hafeez and R. Mahmood, *J. Water Reuse Desalin.*, **10**, 70 (2020);
https://doi.org/10.2166/wrd.2020.054

21. K. Sukla Baidya and U. Kumar, *S. Afr. J. Chem. Eng.*, **35**, 33 (2021);
https://doi.org/10.1016/j.sajce.2020.11.001

22. R.A.E.G. Mansour, M.G. Simeda and A.A. Zaatout, *RSC Adv.*, **11**, 7851 (2021);
https://doi.org/10.1039/D0RA08488C

23. A. Sharma and R. Anthal, *Appl. Water Sci.*, **12**, 1 (2022);
https://doi.org/10.1007/s13201-021-01536-9

24. M. Abbas, *Adsorpt. Sci. Technol.*, **38**, 464 (2020);
https://doi.org/10.1177/0263617420957829

25. Z. Heidarinejad, M.H. Dehghani, M. Heidari, G. Javedan, I. Ali and M. Sillanpää, *Environ. Chem. Lett.*, **18**, 393–415 (2020);
https://doi.org/10.1007/s10311-019-00955-0

26. M.S. Bretanha, G.L. Dotto, J.C.P. Vaghetti, S.L.P. Dias, E.C. Lima and F.A. Pavan, *Desalination Water Treat.*, **57**, 28474 (2016);
https://doi.org/10.1080/19443994.2016.1179223

27. A.F. Ali, A.S. Kovo and S.A. Adetunji, *J. Encapsulation Adsorpt. Sci.*, **7**, 95 (2017);
https://doi.org/10.4236/jeas.2017.72007

28. A. Ragab, I. Ahmed and D. Bader, *Molecules*, **24**, 847 (2019);
https://doi.org/10.3390/molecules24050847

29. V. Yadav, D.P. Tiwari and M. Bhagat, *Int. J. Res. Anal. Rev.*, **6**, 958 (2019).

30. C. Bläker, J. Muthmann, C. Pasel and D. Bathen, *ChemBioEng*, **6**, 119 (2019);
https://doi.org/10.1002/cben.201900008

31. J.O. Ighalo and A.G. Adeniyi, *SN Appl. Sci.*, **2**, 509 (2020);
https://doi.org/10.1007/s42452-020-2335-x

32. V. Yadav, D.P. Tiwari and M. Bhagat, *Desalination Water Treat.*, **184**, 214 (2020);
https://doi.org/10.5004/dwt.2020.25369

33. K. Singh, M. Gautam, B. Chandra and A. Kumar, *Desalination Water Treat.*, **57**, 24487 (2016);
https://doi.org/10.1080/19443994.2016.1141328

34. A. Yadav, M. Bhagat and V. Yadav, *Int. J. Eng. Tech. Sci. Resch.*, **4**, 149 (2017).

35. V. Yadav, D.P. Tiwari and M. Bhagat, *Int. J. Basic Appl. Res.*, **9**, 1282 (2019).

36. M. Bhagat, A. Yadav and V. Yadav, *Int. J. Res. Advent Technol.*, **6**, 688 (2018).

37. R.A. Mansour, A. El Shahawy, A. Attia and M.S. Beheary, *Int. J. Chem. Eng.*, **2020**, 1 (2020);
https://doi.org/10.1155/2020/8053828

38. V. Yadav, D.P. Tiwari and M. Bhagat, *Indian Chem. Eng.*, **63**, 1 (2019);
https://doi.org/10.1080/00194506.2019.1684212

39. R.M.M. Santos, R.G.L. Gonçalves, V.R.L. Constantino, C.V. Santilli, P.D. Borges, J. Tronto and F.G. Pinto, *Appl. Clay Sci.*, **140**, 132 (2017);
https://doi.org/10.1016/j.clay.2017.02.005

40. M. Fazlzadeh, R. Khosravi and A. Zarei, *Ecol. Eng.*, **103**, 180 (2017);
https://doi.org/10.1016/j.ecoleng.2017.02.052

41. J. Fu, Z. Chen, M. Wang, S. Liu, J. Zhang, J. Zhang, R. Han and Q. Xu, *Chem. Eng. J.*, **259**, 53 (2015);
https://doi.org/10.1016/j.cej.2014.07.101

42. R.L. Liu, Y. Liu, X.Y. Zhou, Z.Q. Zhang, J. Zhang and F.Q. Dang, *Bioresour. Technol.*, **154**, 138 (2014);
https://doi.org/10.1016/j.biortech.2013.12.034

43. Y. Kismir and A.Z. Aroguz, *Chem. Eng. J.*, **172**, 199 (2011);
https://doi.org/10.1016/j.cej.2011.05.090

44. M. Ghaedi, H. Hossainian, M. Montazerozohori, A. Shokrollahi, F. Shojaipour, M. Soylak and M.K. Purkait, *Desalination*, **281**, 226 (2011);
https://doi.org/10.1016/j.desal.2011.07.068

45. V.S. Mane and P.V.V. Babu, *Desalination*, **273**, 321 (2011);
https://doi.org/10.1016/j.desal.2011.01.049

46. B.K. Nandi, A. Goswami and M.K. Purkait, *J. Hazard. Mater.*, **161**, 387 (2009);
https://doi.org/10.1016/j.jhazmat.2008.03.110

47. L.T. Popoola, T.A. Aderibigbe, A.S. Yusuff and M.M. Munir, *Environ. Qual. Manage.*, **28**, 63 (2018);
https://doi.org/10.1002/tqem.21597